# Spectroscopic Evidence for a Conformational Transition in Horseradish Peroxidase at Very Low pH†

Giulietta Smulevich,*,‡ Mauro Paoli,‡ Giampiero De Sanctis,§ Anna Rita Mantini,‡ Franca Ascoli,|| and Massimo Coletta*,§

*Dipartimento di Chimica, Università di Firenze, Via G. Capponi 9, 50121 Firenze, Italy, Dipartimento di Biologia Molecolare, Cellulare ed Animale, Università di Camerino, Via F. Camerini 2, 62032 Camerino (MC), Italy, and Dipartimento di Medicina Sperimentale e Scienze Biochimiche, Università di Roma Tor Vergata, Via di Tor Vergata 135, 00133 Roma, Italy*

*Received February 21, 1996; Revised Manuscript Received September 18, 1996*⊗

ABSTRACT: Resonance Raman (RR), electronic absorption, and circular dichroism (CD) spectroscopies of the ferric, ferrous, and ferrous−CO forms of horseradish peroxidase (HRP-C) at pH 3.1 are reported. The CD spectra in the UV region show only a small decrease in the α-helical content upon pH lowering, whereas dramatic changes are observed in the Soret region. The final form of ferric HRP-C is 5-coordinate high-spin heme whose histidine ligand is replaced by a water ligand with a polar character. The electronic and CD spectra show the presence of an intermediate form with a 6-coordinate heme. Therefore, the cleavage of the proximal Fe−imidazole bond is preceded by the binding of a distal water molecule. For the ferrous form of HRP-C, the pH-dependence of the absorption spectra revealed only the native form in the range pH 5−7 and an unfolded form with a Soret maximum at 383 nm at pH 3.1. An intermediate state, characterized by a Soret maximum at 424 nm, was observed only in a transient way, within a few milliseconds. A metastable and a final species are observed also for the ferrous−CO complex at pH 3.1, as proved by isosbestic points in the electronic absorption spectra. The two forms show different RR $\nu$(Fe−C) and IR $\nu$(CO) modes. The metastable form corresponds to a heme where histidine is replaced by water. The final form is due to the displacement of the water ligand by the proximal histidine. We propose a kinetic model to account for our results at pH 3.1 for the ferric, ferrous, and ferrous−CO forms.

Peroxidases are a class of hemoproteins, which in the ferric form catalyze several important reactions, such as oxidation by hydrogen peroxide of a wide range of substrates, namely cytochrome *c*, substituted phenols, and some of the more negative methoxybenzenes (Sakurada et al., 1990; Kersten et al., 1990). However, they are also able to reversibly bind exogenous ligands of the heme iron, such as CO, NO, and isonitriles in the reduced forms, and cyanide, fluoride, and azide in the oxidized form.

The two best characterized peroxidases are cytochrome *c* peroxidase (CCP)[1] (Bosshard et al., 1991) and horseradish peroxidase C (HRP-C) (Dunford, 1991), which both display a very fast kinetic behavior with ligands of the ferric form (Morishima et al., 1978). However, in the ferrous form an unusually slow kinetic behavior is observed for CO binding (Kertesz et al., 1965; Coletta et al., 1986), suggesting that the redox equilibrium may be accompanied by a marked conformational change which brings about a relevant enhancement of the free energy barrier for ligand interaction in the ferrous form. Such a feature appears evident both in the association and dissociation rate constants for CO binding, and it has been shown that in HRP-C pH lowering induces a dramatic increase for the kinetic CO dissociation process without affecting to a significant extent the CO association rate constant (Coletta et al., 1986). On the other hand, upon raising the pH to 10 an enhancement for both kinetic parameters can be observed (Iizuka et al., 1985; Coletta et al., 1986).

The occurrence of an "alkaline" proton-linked conformational change in ferrous HRP-C with a p$K_a \approx 7.5$ has been reported previously (Yamada & Yamazaki, 1975; Smith et al., 1983; Sharonov et al., 1988), and it appears to be accompanied by an increase of CO-binding second-order rate constant as pH is raised (Kertesz et al., 1965; Coletta et al., 1986). A similar behavior is observed in CCP (Iizuka et al., 1985), and recent data on the CO-binding behavior of wild type CCP and its mutants in different positions around the heme indicate that the pH-dependence of CO binding is altered when His181 is substituted by Gly, suggesting that (at least) one of the protons involved stems from His181 and its interaction with propionates (Miller et al., 1990a,b). In addition, distal Arg48 appears to influence in CCP only the CO dissociation rate constant through an alteration of the interaction of the heme with the proximal imidazole ligand (Miller et al., 1990b), suggesting a close energetic interaction between the distal and the proximal portions of the heme pocket in CCP, which is not observed in other monomeric hemoproteins. A recent study on CO-binding

† This work was supported by the Italian Consiglio Nazionale delle Ricerche (CNR) (to G.S and M.C.) and The Ministero Università e Ricerca Scientifica e Tecnologica (MURST) (to G.S.).

* Authors to whom correspondence should be addressed. E-mail: G.S., SMULEV@CHIM.UNIFI.IT; M.C., COLETTA@CAMBIO.UNICAM.IT.

‡ Università di Firenze.

§ Università di Camerino.

|| Università di Roma Tor Vergata.

⊗ Abstract published in *Advance ACS Abstracts,* December 15, 1996.

[1] Abbreviations: 5-c and 6-c, 5- and 6-coordinate; HS and LS, high and low spin; CD, circular dichroism; RR, resonance Raman; NMR, nuclear magnetic resonance; CCP, cytochrome *c* peroxidase; HRP-C, horseradish peroxidase isoenzyme C; Mb, myoglobin; wt, wild type.

S0006-2960(96)00427-8 CCC: $14.00 

properties of HRP-C mutants (Meunier et al., 1995) has been carried out only at pH 8.5. Therefore, it is not enough to allow a detailed comparison between CCP and HRP-C for the modulation of CO-binding mechanism. However, these two peroxidases display a closely similar pH-dependence for CO dissociation kinetics (Coletta et al., 1986), which suggests that the interaction between distal and proximal portions observed in CCP should be present in HRP-C as well.

Even more peculiar appears the additional pH-dependent transition of HRP-C in the acid region, which is characterized by an unusual dynamic behavior, the pH effect being exerted only on the CO dissociation process (Coletta et al., 1986). Thus, in all other monomeric hemoproteins observed up to now, pH lowering brings about a dramatic enhancement of CO association rate constants (Coletta et al., 1985), which has been correlated to the cleavage (or severe weakening) of the proximal bond and to the consequent reduction of the free energy barrier determined by the release of the conformational constraints induced by the Fe−His bond. Therefore, the lack of a rate increase for CO association to HRP-C and CCP upon pH lowering, even in the presence of a protonation of the $N_\epsilon$ of the proximal imidazole ring, and thus the cleavage (or severe weakening) of the proximal Fe−His bond (Ascenzi et al., 1989), indicates that proximal constraints are less important in modulating the CO association kinetic behavior of peroxidases; and recent data on CO binding to HRP-C mutated in some residues of the distal portion of the heme pocket (Meunier et al., 1995) indeed confirm that, unlike other hemoproteins, CO binding to HRP-C is completely controlled by the ligand access through the distal barrier, at least at pH 8.5.

However, a different modulation mechanism must be responsible for the pH-dependence of the CO dissociation (Coletta et al., 1986), and no such study has been performed as yet on HRP-C mutant. On the basis of these considerations, we have carried out an investigation on the conformational change in HRP upon lowering the pH to 3.1. Such a transition has been followed by electronic absorption, circular dichroism, and resonance Raman spectroscopies, aiming to the formulation of a comprehensive mechanism which may account for the observed spectroscopic and functional features.

## MATERIALS AND METHODS

Horseradish peroxidase isoenzyme C (HRP-C) was purchased from Sigma (type VI, RZ = 3.2, activity 325 Units/mg of solid) and purified as previously described (Smulevich et al., 1991).

The pH was adjusted with 0.1 M phosphate (pH 6−7), 0.1 M citrate (pH 5−3), and 0.3 and 0.5 M phosphate buffer (pH 3.5−3.1). For this latter case the pH was brought down to pH 3.1 with either phosphoric acid or HCl. In order to have a constant ionic strength at this acid pH, all measurements have been carried out in the presence of 0.5 M NaCl.

The ferrous form was prepared by adding a minimum volume of fresh sodium dithionite solution to the degassed buffered solution. Sample concentration was determined spectrophotometrically using an extinction coefficient of 102 $cm^{-1}$ $mM^{-1}$ at 403 nm, was 0.1−0.4 mM of enzyme for RR spectra, and was 10 times more diluted for UV−visible absorption spectra. The CO adducts at acid pH were obtained by gently flowing CO (1 atm) (Rivoira) from a gas cylinder over the surface of the ferric protein, which was then reduced with dithionite, whereas at pH 7 the gas was introduced over the surface of the reduced protein. The $^{13}CO$ (99%) adducts were obtained by introducing the gas (Matheson) over the HRP-C solution in an evacuated NMR tube.

Absorption spectra were measured with a Cary 5 and a Cary 14 spectrophotometer. Absorption spectra were measured both prior to and after Raman experiment, and no degradation was detected under the experimental conditions applied in this study. Infrared spectra were recorded at 25 °C with a Bruker 1F20HR FTIR spectrophotometer. The CO complexes were transferred by a gas-tight syringe flushed with CO into a $CaF_2$ IR cell (0.1 mm path length) which had been previously flushed with CO. The corresponding buffer solution was used as reference.

The RR spectra were obtained by excitation with the 406.7, 413.1, and 530.9 nm lines of a $Kr^+$ laser (Coherent, Innova 90/K) and the 457.9, 496.5, and 514.5 nm lines of an $Ar^+$ laser (Coherent, Innova 90/5). The back-scattered light from a slowly rotating NMR tube was collected and focused into a computer-controlled double monochromator (Jobin-Yvon HG 2S), equipped with a cooled photomultiplier (RCA C31034 A) and photon-counting electronics. The RR spectra were calibrated with indene and $CCl_4$ as standards to an accuracy of 1 $cm^{-1}$ for intense isolated bands.

The electronic absorption, IR, and RR spectra were collected at room temperature, i.e., about 23 °C, unless differently stated.

Polarized RR spectra were obtained by inserting a polaroid analyzer between the sample and the entrance slit of the spectrometer. The depolarization ratios, $\rho$, of the bands at 314 and 460 $cm^{-1}$ of $CCl_4$ were measured to check the reliability of the polarization measurements using a rotating NMR tube with 180° back-scattered geometry. The values obtained, 0.73 and 0.01, compared favorably with the theoretical values of 0.75 and 0.00, respectively.

Low temperature was obtained using a closed-cycle He cryotip with an automatic temperature control. The RR spectra were measured after transferring the protein solutions with a gas-tight syringe to a small groove in the copper cold finger of the cryostat at 180 K under nitrogen flow. The temperature was then slowly decreased to 13 K under vacuum, and RR spectra were obtained at this temperature as well as at intermediate temperatures.

Kinetic experiments have been carried out at the Department of Biochemical Sciences of the University of Rome "La Sapienza" on a Gibson-Durrum stopped-flow apparatus with a 2 cm path length observation cell and interfaced to a desktop computer for data acquisition (On Line System, Jefferson, GA). Transient spectra of unliganded ferrous HRP-C have been obtained by mixing reduced deoxygenated HRP at pH 6.0 in a low ionic strength buffer ($I$ = 2 mM) with an accurately degassed buffer at high ionic strength to give a final pH 3.1. The spectra have been calculated by the amplitudes at different wavelengths of the process which was leading to the final spectrum at about 10 s after mixing.

Circular dichroism spectra in the UV and Soret regions were carried out at 20 °C in a 10 or 2 mm path length quartz cell in a Jasco J710 spectropolarimeter. Molar ellipticity ($\theta$) (deg·$cm^2$·$dmol^{-1}$) is expressed on a heme concentration basis (in the Soret region) and on a mean residue concentration basis (in the UV region).

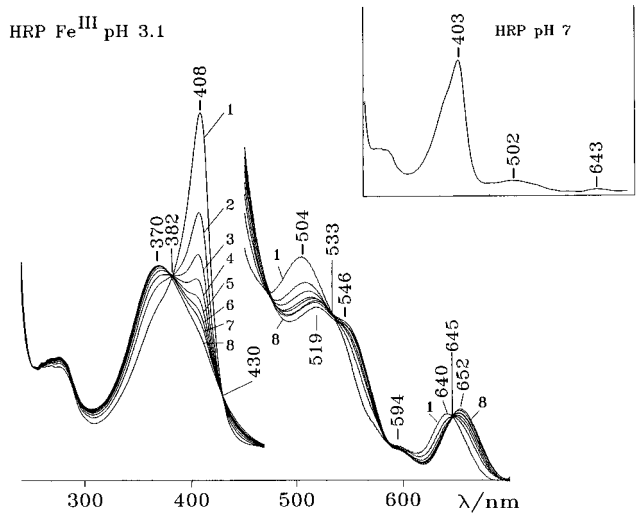


FIGURE 1: Electronic absorption spectra of HRP-C at pH 3.1 in phosphate buffer 0.5 M $Cl^-$ as function of time: 1, recorded immediately after preparation; 2, after 4 min; 3, after 8 min; 4, after 11 min; 5, after 13 min; 6, after 16 min; 7, after 20 min; and 8, after 30 min. In the inset is reported the spectrum obtained readjusting the pH from 3.1 to 7.0 by adding NaOH. Scan-speed 300 nm/min. The visible region has been expanded by 3 times.

## RESULTS

*Ferric HRP*. Figure 1 shows the absorption spectra of ferric HRP-C at pH 3.1, obtained in the presence of $Cl^-$ ion, as a function of time. The inset shows the absorption spectrum obtained readjusting the pH from 3.1 to 7 by adding NaOH. This spectrum is identical to that obtained by directly dissolving the protein in phosphate buffer at pH 7. Therefore, the acid transition is completely reversible and the protein is not denatured. From Figure 1 it can be seen that the spectrum obtained immediately after preparation (spectrum 1) has a Soret at 408 nm and a $\beta$ band at 504 nm, both red-shifted as compared to pH 7, whereas the charge-transfer band is at 640 nm, 3 nm blue-shifted with respect to pH 7. Upon time new bands at 370 and 519 nm increase at the expense of the bands at 408 and 504 nm respectively, with well-defined isosbestic points at about 382, 430, and 533 nm, indicating the conversion from one species to another. Furthermore, the band at 640 nm red-shifts to 652 nm with an isosbestic point at 645 nm. This latter band grows with time (see Figure 1). After 30 min (spectrum 8) no further changes were observed and in the Soret region a weak shoulder at about 405 nm is still present, suggesting that at this pH some protein keeps a conformation similar to that obtained at pH 7.0, or to the initial form observed at pH 3.1. In the corresponding experiments carried out at pH 3.1 without $Cl^-$ ion, the rate is slower and the final spectrum is characterized by two broad bands in the Soret region with a maximum at 370 nm and a pronounced shoulder at about 408 nm and in the CT1 region with a maximum at 640 nm and a shoulder at about 652 nm (data not shown).

Circular dichroism (CD) spectra in the UV (Figure 2, left) and in the Soret region (Figure 2, right) indicate that over the same time interval there is only a small decrease in the α-helical content of ferric HRP upon lowering to pH 3.1 (see Figure 2, left). On the other hand, in the Soret region on pH lowering there is an immediate red-shift of the peak ellipticity (like in the case of peak absorption, see Figure 1), accompanied within the first 30 min by a slow decrease of ellipticity, which never fades out (see Figure 2, right).

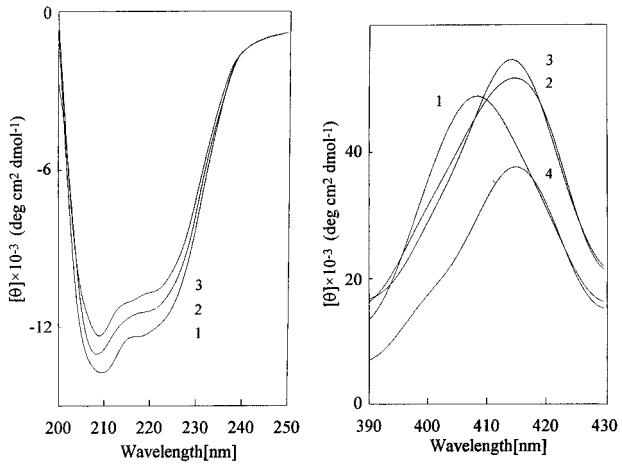


FIGURE 2: (left) Far-UV CD spectra of ferric HRP-C as a function of time after mixing with low-pH buffer (final pH 3.1). [$\theta$] is expressed as a mean residue concentration. Spectrum 1 is ferric HRP-C at pH 7. Spectra 2 and 3 correspond to ferric HRP-C at pH 3.1 after 1 min and 60 min, respectively. (right) Soret CD spectra of ferric HRP-C as a function of time after mixing with low-pH buffer (final pH 3.1). [$\theta$] is expressed as heme concentration. Spectrum 1 is ferric HRP-C at pH 7. Spectra 2−4 correspond to ferric HRP-C at pH 3.1 after 1 min, 2 min, and 30 min, respectively. For further details, see text.

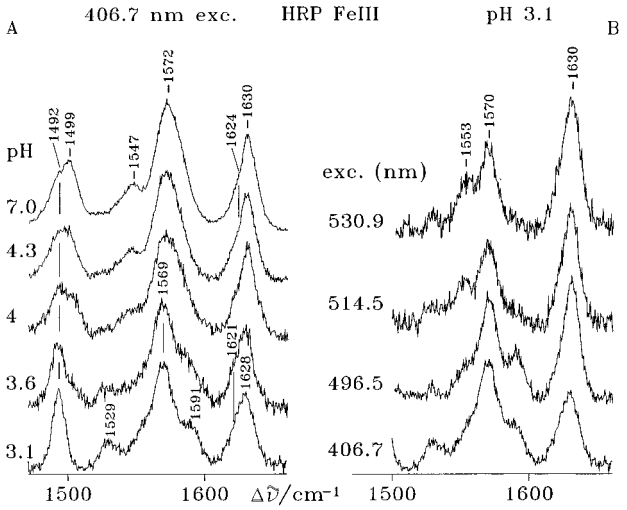


FIGURE 3: (A) RR spectra of HRP-C taken at various pHs with 406.7 nm excitation. Experimental conditions: 5 $cm^{-1}$ resolution; 40 mW laser power at the sample; pH 3.1, 4 s/0.5 $cm^{-1}$; pH 3.6, 5 s/0.5 $cm^{-1}$, pH 4 and 4.3, 3 s/0.5 $cm^{-1}$, and pH 7.0, 1 s/0.5 $cm^{-1}$. (B) RR spectra of HRP-C taken at pH 3.1 with different excitation wavelengths. Experimental conditions: 5 $cm^{-1}$ resolution; 406.7 nm, 40 mW laser power at the sample; 4 s/0.5 $cm^{-1}$; 496.5 nm, 40 mW laser power at the sample; 40 s/0.5 $cm^{-1}$; 514.5 nm, 80 mW laser power at the sample; 5 s/0.5 $cm^{-1}$; 530.9 nm, 40 mW laser power at the sample; 50 s/0.5 $cm^{-1}$.

Figure 3 shows the RR spectra in the high-frequency region of HRP taken at different pH values (A). The spectrum at pH 3.1 was recorded 30 min after the preparation, and it should be correlated with the absorption spectrum 8 of Figure 1 and the CD spectrum 4 of Figure 2, right. At pH 7 HRP-C showed the coexistence of two high-spin species (Smulevich et al., 1994). Upon lowering the pH, the RR spectra show gradual intensity and frequency variations. At pH 3.1 a new species appears, characterized by bands at 1492, 1529, 1569, 1591, 1621 (sh), and 1628 $cm^{-1}$. In order to assign these bands, we undertook a study using different excitation wavelengths (Figure 3B) and in polarized light (data not shown). With Soret excitation,

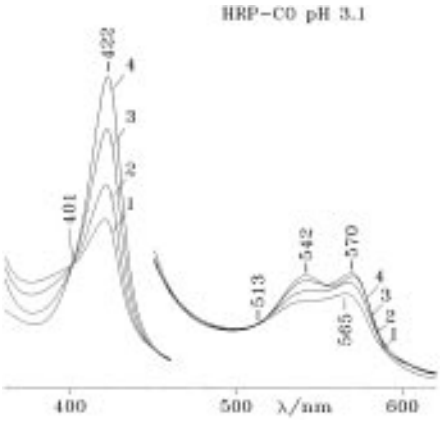


FIGURE 4: Electronic absorption spectra of HRP−C/CO complex at pH 3.1 in phosphate buffer 0.5 M as function of time: 1, after 2 min; 2, after 4 min; 3, after 10 min; 4, after 90 min. Scan-rate 300 nm/min. The visible region has been expanded by 3 times.

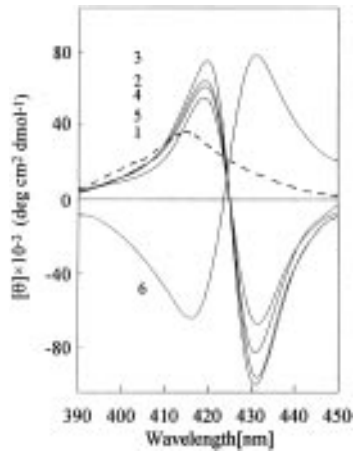


FIGURE 5: Soret CD spectra of CO derivative of ferrous HRP-C as a function of time after mixing ferric HRP-C at pH 3.1 with CO saturated buffer at the same pH containing sodium ditionite (20 mg/mL final concentration). [$\theta$] is expressed as heme concentration. Spectrum 1 (dashed line) is ferric HRP-C after 30 min at pH 3.1. Spectra 2−5 correspond to HRP-C/CO after 1 min, 5 min, 30 min, and 60 min, respectively, after reduction under CO atmosphere. Spectrum 6 corresponds to HRP-C/CO at pH 7. For further details, see text.

polarized bands, due to the totally symmetric modes, and the $\nu$(C=C) vinyl stretching modes are enhanced via the Albrecht's A-term. The non-totally symmetric modes of the $B_{1g}$ species, observed also in the Soret excitation via the Jahn−Teller mechanism, together with the inverse polarized bands of $A_{2g}$ species, are selectively enhanced via B-term mechanism in Q band excitation. Based on their depolarization ratios and excitation profiles, the bands were assigned as follows: $\nu_4$ at 1372 cm$^{-1}$, $\nu_3$ at 1492 cm$^{-1}$, $\nu_{38}$ at 1529 cm$^{-1}$, $\nu_{11}$ at 1553 cm$^{-1}$, $\nu_2$ at 1569 cm$^{-1}$, $\nu_{19}$ at 1570 cm$^{-1}$, $\nu_{37}$ at 1591 cm$^{-1}$, $\nu_{10}$ at 1630 cm$^{-1}$, $\nu$(C=C) vinyl stretching modes at 1621 and 1628 cm$^{-1}$, respectively.

*HRP−CO.* Figure 4 shows the absorption spectra of the complex $Fe^{II}$ HRP−CO at pH 3.1 as a function of time. The spectrum of the freshly prepared sample (after 2 min) shows a broad band in the Soret region with a maximum at 422 nm and a shoulder at about 395 nm. Also, the Q region is characterized by a broad band with a maximum at 565 nm ($\alpha$ band) and a shoulder at shorter wavelength. Upon time the band at 422 nm grows in and the shoulder decreases in intensity, while in the Q band region two maxima at 542 ($\beta$ band) and at 570 nm ($\alpha$ band) occur. Isosbestic points at 401 and 513 nm are observed, indicating the conversion from one species to another. After 90 min from the preparation no further changes were observed.

Figure 5 shows the experiment followed by CD spectroscopy in the Soret region. From data in the UV (data not shown) it becomes evident, as for the ferric form, that pH lowering to 3.1 does not bring about a relevant decrease of $\alpha$-helical content, suggesting that acidification of HRP−CO leaves the secondary structure of the protein unaltered. On the other hand, in the Soret region the CD spectra of HRP−CO at pH 3.1 display features significantly different from those observed at neutral pH. Thus, while at pH 7.0 the spectrum displays a positive ellipticity peak at $\lambda \approx 432$ nm and a negative peak at $\lambda \approx 417$ nm (see spectrum 6 in Figure 5), at pH 3.1 HRP−CO shows an inversion of ellipticity with a negative peak at $\lambda \approx 433$ nm and a positive ellipticity at $\lambda \approx 420$ nm, a feature which appears immediately and remains unchanged for several hours (see spectra 2−5 in Figure 5). The inversion in ellipticity, which reflects a change in the relative orientation of the dipole electric and magnetic moments for the $\pi \rightarrow \pi^*$ heme transition (Willick et al., 1969), indeed is indicative of a variation of the heme environment of HRP−CO upon lowering pH to 3.1. It must

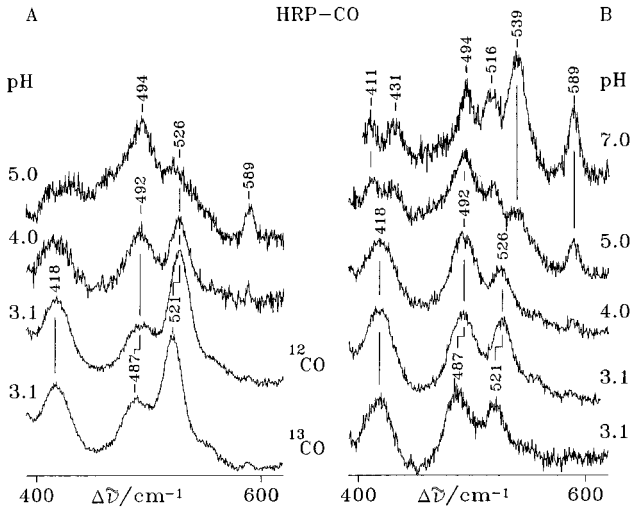


FIGURE 6: RR spectra of HRP-C/CO and $^{13}$CO complexes taken at various pHs with 406.7 nm (A) and 413.1nm (B) excitation. Experimental conditions: 5 cm$^{-1}$ resolution; (A) pH 3.1, 25 mW laser power at the sample, ($^{13}$CO) 5 s/0.5 cm$^{-1}$ and (CO) 10 s/0.5 cm$^{-1}$; pH 4, 35 mW at the sample, 6 s/0.5 cm$^{-1}$; pH 5.0, 10 mW at the sample, 35 s/0.5 cm$^{-1}$; (B) pH 3.1, ($^{13}$CO) 30 mW laser power at the sample, 8 s/0.5 cm$^{-1}$; (CO) 8 mW laser power at the sample, 18 s/0.5 cm$^{-1}$; pH 4.0, 10 mW laser power at the sample, 14 s/0.5 cm$^{-1}$; pH 5.0, 10 mW laser power at the sample, 25 s/0.5 cm$^{-1}$; pH 7.0, 5 mW at the sample, 40 s/0.5 cm$^{-1}$.

be outlined that if the CO adduct is formed at pH 7.0 and then the pH is brought to 3.1, there is a slow transition, from the spectrum observed at neutral pH to the one reported in Figure 5 at pH 3.1, that is completed in about 1 h (data not shown). However, for pH >3.1 the transition is uncomplete, and at pH 3.5 it does not take place [see Coletta et al. (1986)]. When CO is added directly to a reduced protein already at pH 3.1, the complete reaction takes place also at higher pH values. Such a behavior seems to indicate that the final form at pH 3.1 is not independent on the procedure followed.

Figure 6 shows the RR spectra in the low-frequency region of the HRP−CO complex at different pH values, taken with 406.7 nm (A) and 413.1 nm (B) excitations. With 413.1 nm excitation it can be seen that the bands at 539 and 516

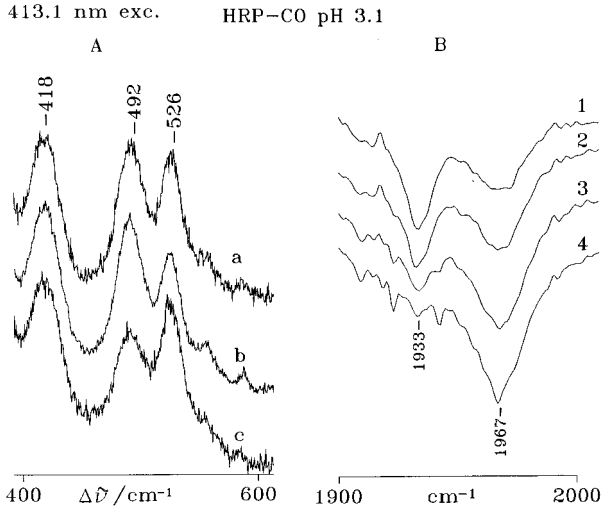


FIGURE 7: RR spectra taken with 413.1 nm excitation (A) and IR spectra (B) of the HRP−CO complex at pH 3.1. (A) Spectra taken in a spinning cell (a) immediately after preparation, (b) 30 min after preparation, and (c) under continuous illumination in a stationary cell. Experimental conditions: 5 $cm^{-1}$ resolution; (a and b) 8 mW laser power at the sample, 18 s/0.5 $cm^{-1}$; (c) 25 mW at the sample, 2 s/$cm^{-1}$ collection interval. (B) IR spectra as function of time: (1) 2 min, (2) 5 min, (3) 20 min, and (4) 60 min after preparation. A total of 32 transients were accumulated for each spectrum (4 $cm^{-1}$ resolution).

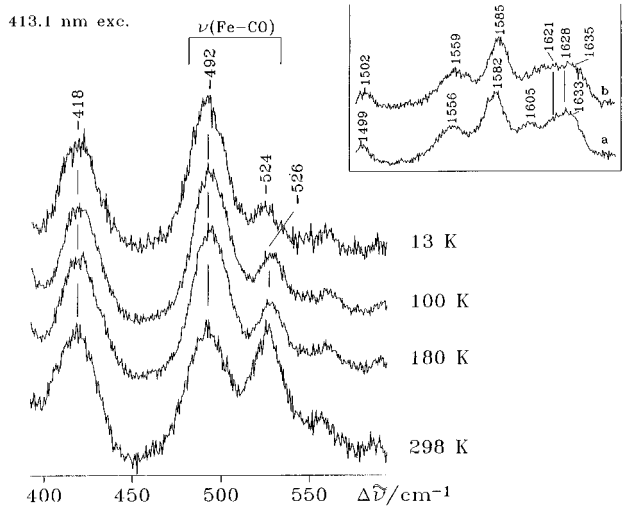


FIGURE 8: Low-frequency RR spectra of HRP-C/CO complex at pH 3.1 taken at various temperatures with 413.1 nm excitation. Experimental conditions: 5 $cm^{-1}$ resolution, 298 K, 30 mW laser power at the sample, 8 s/$cm^{-1}$; from 180 to 13 K, 5 mW laser power at the sample and 5 s/$cm^{-1}$ collection interval. The inset shows the high-frequency region of the corresponding spectra taken at (a) 298 K and (b) 180 K. Experimental conditions as for the low-frequency region, but (a) 10 s and (b) 2 s accumulation.

$cm^{-1}$ observed at pH 7, assigned to two $\nu$(Fe−CO) stretching modes (Uno et al., 1987, Evangelista-Kirkup et al., 1986), decrease in intensity at pH 5 and are replaced by a new band at 526 $cm^{-1}$ upon further lowering of the pH. On the other hand, the band at 494 $cm^{-1}$ assigned to another $\nu$(Fe−CO) stretching mode (Evangelista-Kirkup et al., 1986) increases in intensity and shifts down by 2 $cm^{-1}$ at acid pH. The RR spectra of the HRP−CO and $^{13}$CO complexes taken with both 413.1 and 406.7 nm excitation (bottom spectra, Figure 6) showed that the bands at 526 and 492 $cm^{-1}$ shift down by 5 $cm^{-1}$ upon isotopic substitution, confirming that they are both due to $\nu$(Fe−CO) stretching modes.

The change of the excitation from 413.1 to 406.7 nm leads to a substantial enhancement of the 526 $cm^{-1}$ band relative to the 492 $cm^{-1}$ band, suggesting that the 526 $cm^{-1}$ band derives its intensity from a Soret band which is blue-shifted with respect to the Soret band (422 nm) corresponding to the stable species.

Figure 7 shows the RR spectra (left) of the HRP−CO complex at pH 3.1 obtained (a) on a freshly prepared sample and (b) after 40 min. It can be seen that the 492 $cm^{-1}$ band grows in at the expense of the 526 $cm^{-1}$ band upon time. These data confirm that the 492 $cm^{-1}$ band arises from the Soret at 422 nm, in agreement with the time-dependent absorption spectra. In addition, as previously reported for the Mb−CO complex at acid pH (Sage et al., 1991b), a substantial increase occurs in the intensity of the band at 526 $cm^{-1}$ relative to the band at 492 $cm^{-1}$ in the spectrum obtained under continuous illumination in a stationary cell (Figure 7, c). Therefore, increasing the band at 526 $cm^{-1}$ upon laser illumination, in the RR experiment it is not possible to obtain a complete conversion from one form to another, as it is instead observed from both the electronic absorption (Figure 4) and IR spectra reported in the right panel (B) of Figure 7. In fact the IR spectra of the HRP−CO complex at pH 3.1 taken upon time indicate that the fresh sample (Figure 7, B, spectrum 1) is characterized by two bands at 1933 and 1967 $cm^{-1}$. Upon time this latter band grows in at the expense of the band at 1933 $cm^{-1}$ (Figure 7, B, spectra 2−4). Therefore, the band at 1933 $cm^{-1}$ is a $\nu$(CO) stretching mode associated with the RR $\nu$(Fe−CO) stretching mode at 526 $cm^{-1}$, and the band at 1967 $cm^{-1}$ is the second $\nu$(CO) stretching mode associated with the RR band at 492 $cm^{-1}$. The growing of the 1967 $cm^{-1}$ band at the expense of the 1933 $cm^{-1}$ was very slow when an unpurified protein was used. Recently, Holzbaur et al. (1996) found only the infrared band at 1934 $cm^{-1}$ for HRP−CO at pH 3 using a protein supplied by Boehringer Mannheim.

Figure 8 shows the RR spectra of the acid HRP−CO complex at different temperatures. It can be seen that upon temperature lowering the species characterized by the 492 $cm^{-1}$ band becomes dominant. Therefore, the band at 492 $cm^{-1}$ is assigned to the stable form which is depopulated under continuous illumination in a stationary cell. In the inset of Figure 8 the comparison of the high-frequency region RR spectra of the HRP−CO complexes obtained (a) at room temperature and (b) at 180 K is reported. The comparison shows, that upon lowering the temperature, the core size marker bands increase their frequency by 3 $cm^{-1}$. The same effect has been previously observed for the alkaline metMb, metHb, and HRP (Feis et al., 1994). For this protein it had been found that lowering the temperature causes a strengthening of the Fe−OH bond and a contraction of the core by about 0.1 Å, as determined by the upshifting of the low-spin $\nu$(Fe−OH) stretching mode and the core size marker bands. Both effects were ascribed to an increase of the packing forces (Feis et al., 1994).

As compared with the corresponding spectrum at neutral pH (not shown), at pH 3.1 the band at 1630 $cm^{-1}$ broadens and decreases in intensity. The spectra in polarized light (not shown) indicate that this spectral change upon acidification is due to the increase of the vinyl $\nu$(C═C) stretching mode at 1621 $cm^{-1}$ at the expense of the vinyl $\nu$(C═C) stretching mode at 1630 $cm^{-1}$.

Table 1: Electronic Absorption Maxima (nm) Observed for 5-c HS Proteins

| proteins | pH | Soret | CT2 | $Q_v$ | $Q_0$ | CT1 | ligand |
|---|---|---|---|---|---|---|---|
| CCP[a] | 7.0 | 408 | | 506 | 534 | 646 | $Im^-$ |
| H64L-Mb[b] | 6.0 | 385 | | 507 | 543 | 641 | Im |
| MetMb[c] | 3.0 | 370[d] | 510 | | 545 | 640 | $H_2O$ |
| HRP-C | 3.1 | 370[d] | 519 | | 546 | 652 | $H_2O\cdots R38^+$ |

[a] Vitello et al., 1992. [b] Ikeda-Saito et al., 1992. [c] Palanappian & Bocian, 1994. [d] The Soret transition can overlap or interact with a nearby lying electronic transition.

## DISCUSSION

*Ferric form*. The final stable form of ferric HRP at pH 3.1 in the presence of 0.5 M NaCl gives rise to electronic absorption and RR spectra similar to those previously observed for metMb at acid pH (Sage et al., 1991a; Palaniappan & Bocian, 1994). The pH-dependence of sperm whale metMb has been examined in detail by means of different spectroscopic methods (Han et al., 1990; Sage et al., 1991a,b; Palaniappan & Bocian, and reference therein, 1994). MetMb shows two forms: (i) the aquo 6-c HS species (N) at neutral pH and (ii) the acid form which has been called U′ by Palaniappan and Bocian and U by Sage et al. (1991a); these latter authors concluded that in the N → U transition the protein has lost an axial ligand. Even if the RR results did not give any direct indication of which ligand has been displaced, the large change in the electronic spectra had been taken as an indication that the breakage of the iron−histidine bond takes place in metMb. Actually, this hypothesis has been recently confirmed by the X-ray structure of MetMb at pH 4.0, which shows that the Fe−histidine bond is elongated (2.5 Å) with respect to the protein at pH 6.0 (2.15 Å) (Yang & Phillips, 1996). Therefore, based on the similarity of the RR spectra between metMb and HRP-C at acid pH, this latter should be in the U-form. The RR spectrum of HRP-C is typical of a 5-c HS species, and the frequencies of the bands are almost identical to those previously reported for metMb (Palaniappan & Bocian, 1994; Sage et al., 1991a).

Also, the electronic absorption spectrum of the U-form of HRP-C is quite similar to that of metMb as the Soret region and the Q bands are concerned. Some differences, however, are observed in the wavelength of the bands at 519 (510 in metMb) and 652 (640 in metMb) nm (Table 1). The origin of the band at 519 (and 510 in metMb) nm is not certain. But considering its anomalous red-shifted maximum with respect to other 5-c HS heme proteins in general, and to HRP-C itself at neutral pH (insert, Figure 1), it could be due to the overlapping contribution of the $\beta$ band with a CT transition (CT2) (Vitello et al., 1993). The bands at 652 nm for HRP-C and 640 nm for metMb should be due to the charge transfer (CT1) from the porphyrin to the iron, via the $\pi(a'_{2u}) \rightarrow d_\pi$ ($e_g$) electronic transition as assigned on the basis of the electronic absorption spectra in polarized light of metMb (pH 7.0, CT1 = 632 nm) and metMbOH (CT1 = 600 nm) single crystals (Eaton & Hochstrasser, 1968). The $a'_{2u}$ level [indicated as $\tau(\pi)$ by Maltempo, 1976] lies at lower energy than the HOMO $a_{2u}$ level, and it has been suggested that the wavelength of this CT band depends on the ligand field strength (the maximum shifts to the red upon increase the ligand field strength) and on the capability of the ligand to donate $\pi$ electrons (a better $\pi$ donor raises in energy the $d_\pi$ orbitals causing a blue-shift of the CT1 band) (Smulevich et al., 1995). The $d_\pi$ orbitals can be raised in energy by interaction with the $\pi$ orbitals of the pyrrole rings and the axial ligands. For the water ligand the $\pi$ interaction is given by the filled p orbitals which are free from chemical bonds. Therefore, the extent of the interaction depends on water ionization being maximum for $OH^-$ intermediate for $H_2O$ and zero for $H_3O^+$. Also hydrogen bonding affects the $\pi$ interaction. In fact, in the case in which $H_2O$ or $H_3O^+$ acts as a hydrogen bond donor, the extent of p donation to the Fe atom depends on the hydrogen bond strength; the stronger the hydrogen bond, the more the oxygen p orbitals are able to interact with the Fe $d_\pi$ orbitals and to raise the energy of the CT transition. Unlike the case in which $H_2O$ or $OH^-$ acts as a hydrogen bond acceptor, the energy of the CT transition decreases with the strength of the hydrogen bond.

Since the proximal imidazole ligand is lost for both proteins at acid pH, the observed red-shift of the CT1 band of HRP with respect to that of metMb (Palaniappan & Bocian, 1994) might be due to a different polarity of the water ligand bound to the heme iron, which is hydrogen-bonded with the distal Arg in the peroxidase. In fact, structural differences between Mb and HRP are detectable both on the distal and on the proximal side of the heme pocket. In particular, one must be reminded of the presence of (i) a positively charged guanidinium group of an Arg residue in the distal portion, which is postulated to inhibit the protonation of the distal His at neutral pH during the catalytic cycle (Poulos & Kraut, 1980; Poulos, 1988), and (ii) an Asp residue in the proximal region, which forms a strong polar hydrogen bond with the $N_\delta$ of the proximal His (La Mar & de Ropp, 1982). In addition, the X-ray structures of different peroxidases show the presence of a hydrogen bond network in the distal cavity connecting various water molecules, distal residues, and the propionyl groups of the heme. Wild type metMb has a water molecule coordinated to the heme iron and hydrogen-bonded to the distal His67. An additional water molecule is located toward the back of the distal pocket within hydrogen-bonding distance of the coordinated water molecule, but too far away for direct interaction with the distal His (Quillin et al., 1992). Recently, high-resolution crystal structure has been determined for different distal histidine mutants of sperm whale Mb in several ligated forms (Quillin et al., 1992, 1993) and the coordination structures of the ferric heme iron have been determined by spectroscopic methods (Morikis et al., 1989; Ikeda-Saito et al., 1992). The results showed that metMb with hydrophobic substitutions at residue 64 (Val and Leu) lacks a water molecule in the sixth position. The corresponding 5-c HS heme is characterized by a Soret maximum at 395 nm and by the CT1 at 641 nm (Ikeda-Saito et al., 1992). The His64 → Gln, Gly, Thr, Val, and Leu substitutions result in a progressive decrease in polarity of the distal cavity. In particular, in the His64Gln mutant the distal water molecule is coordinated to the heme iron and no evidence was found for a second water molecule in the distal pocket. The electronic absorption spectrum is characteristic of a predominant 6-c HS heme, but the missing hydrogen bond with the distal His brings about a red-shift of the CT1 band by 4 nm (637 vs 633 in the wild type) (Ikeda-Saito, et al., 1992) (Table 2).

The most striking difference in the absorption spectra of HRP-C, compared with metMb, is the presence of an

Table 2: Electronic Absorption Maxima (nm) Observed for 6-c HS Proteins

| proteins | pH | Soret | CT2 | $Q_v$ | $Q_0$ | CT1 | ligands |
|---|---|---|---|---|---|---|---|
| MetMb[a] | 7.0 | 409 | 504 | | | 633 | Im/$H_2O$···H67 |
| H64Q-Mb[a] | 6.0 | 409 | 506 | | | 637 | Im/$OH_2$ |
| HRP-C | 3.1 | 408 | 504 | | | 640 | Im/$H_2O$···R38$^+$ |
| metMb[b] | 10.4 | 413 | 485 | 543 | 583 | 600 | Im/$OH^-$ |

[a] Ikeda-Saito, 1992. [b] Feis et al., 1994.

intermediate species, characterized by a Soret band at 408 nm, $\beta$ and $\alpha$ bands at 504 and 532 (shoulder) nm, and the CT1 band at 640 nm (Table 2). This spectrum resembles that of the His64 → Gln mutant of Mb (Ikeda-Saito et al., 1992). Therefore, in HRP-C it seems that the cleavage of the proximal Im−Fe bond is preceded by the binding of a distal water molecule with the formation of an intermediate species which slowly converts (in about 30 min) to the final form. The crystal structure of HRP-C has not been yet resolved, but evidence of the presence of distal water molecules has been shown by RR spectra. In fact, at neutral pH this protein is a mixture of 5- and 6-c HS hemes (Smulevich et al., and references therein, 1994). Without $Cl^-$ ions the electronic absorption spectra revealed the presence of two forms: one corresponds to the U-form and, the other could be due either to the intermediate aquo 6-c HS heme or to the species occurring at neutral pH.

*Ferrous form.* The pH-dependence of deoxy sperm whale Mb has been examined in detail by means of different spectroscopic methods (Han et al., 1990; Sage et al., 1991a,b; Palaniappan & Bocian, and reference therein, 1994). Many different forms have been detected. The data indicate the presence of the native form (N) between pH 7 and 4.5, an intermediate (I′) form in the pH 3.5−4.5 range, and the unfolded (U′) form which occurs in the pH 2.6−3.5 range. These forms, characterized by RR spectroscopy, have been identified as a 5-c HS with the proximal histidine bound to Fe atom (N), a 5-c HS, where the fifth ligand is a relatively strongly bound, exchangeable water molecule (I′), and a tetracoordinate heme (U′) (Palaniappan & Bocian, 1994; Sage et al., 1991a), or as a 6-c HS species with very weak axial ligands (Palaniappan & Bocian, 1994). For HRP the pH-dependence of the absorption spectra revealed only the native form (N) in the range of pH between 5 and 7 and the unfolded form (U′) with a Soret maximum at 383 nm at pH 3.1; the I′ form has been possibly observed in a transient way, within few milliseconds after bringing ferrous HRP to pH 3.1 in a rapid-mixing apparatus. The transient spectrum (Figure 9) displays a peak absorption centered at about 424 nm, closely similar to what was observed for deoxy Mb at low pH (Giacometti et al., 1977; Han et al., 1990; Palaniappan & Bocian, 1994), and it converts within a few seconds to a form characterized by a broad band with a peak absorption at about 383 nm (see Figure 9). The similarity of the behavior observed in ferrous HRP with respect to what was reported for deoxy Mb under the same conditions leads to interpret the transient spectrum of ferrous HRP at 424 nm as a form displaying a weak fifth axial ligand (i.e., heme−$H_2O$), which undergoes a transition toward a four-coordinated heme or a hexacoordinated form with two weak ligands (i.e., $H_2O$−heme−$H_2O$, see Palaniappan & Bocian, 1994).

*HRP−CO complex.* As above for the ferric form, the complex with CO at acid pH shows as well the occurrence

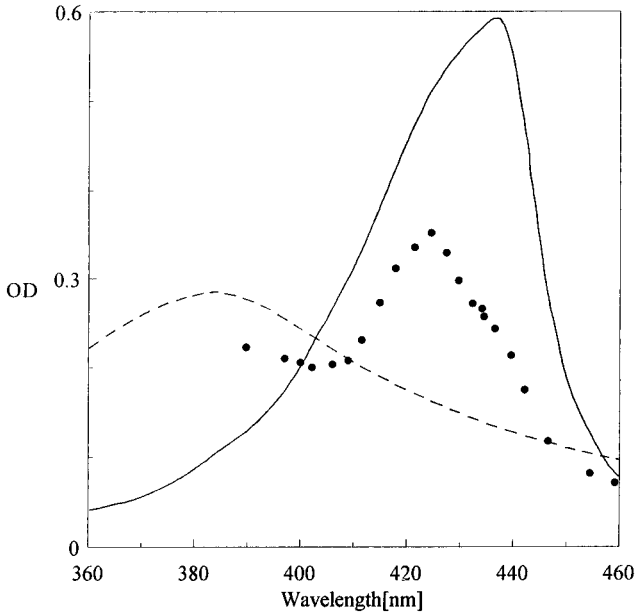


FIGURE 9: Electronic absorption spectrum of unligated ferrous HRP-C (8 $\mu$M heme concentration) at pH 7 (continuous line), after 1 min at pH 3.1 (dashed line), and the transient spectrum (experimental points) obtained 5 ms after mixing unligated ferrous HRP-C at pH 7 with buffer at low pH (final pH 3.1). For further details, see text.

of a metastable form, which appears immediately after the reduction of the ferric species at pH 3.1 in the presence of CO. This metastable form converts then to a stable form at a rate which displays some pH-dependence, being faster at pH 3.1 than at pH 3.3 (data not shown), but no dependence on CO concentration over the range 0.04−0.5 mM. Such a lack of CO concentration dependence indicates that at acid pH along the pathway between the initial ferric form and the final stable CO-bound species there is at least one rate-limiting step slower than the bimolecular CO-binding process itself, which was independently determined [see Coletta et al. (1986) and Ascenzi et al. (1989)]. The absorption spectrum of the metastable form obtained immediately (i.e., within a few tens of seconds) after the preparation of the CO complex from the ferric species displays the presence of two forms in equilibrium with a clear isosbestic point in the Soret region at 401 nm (see Figure 4). The final stable form is characterized by an absorption spectrum similar to that previously reported at neutral pH (Blumberg et al., 1968), suggesting that it is a His−heme−CO complex. As far as the metastable form is concerned, its actual Soret band maximum cannot be determined exactly, but it is important to remark that the replacement of His by $H_2O$ in the His−protoheme−CO complex gives rise to a Soret band at 405 nm (Rougee & Brault, 1973; Wang & Brinigar, 1979), and a further ∼10 nm blue-shift is expected for a 5-c protoheme−CO complex (Brault & Rougee, 1974; Traylor et al., 1985; Cannon et al., 1976; Sage et al., 1991a). However, the visible region of the spectrum of a 5-c protoheme−CO complex is very peculiar, being characterized by an extremely strong $\alpha$ band at 544 nm, whereas for the 6-c $H_2O$−protoheme−CO complex the $\alpha$ and $\beta$ bands are around 525 and 560 nm, respectively, with a similar intensity (Rougee & Brault, 1973). The spectrum of the metastable CO adduct reported in Figure 4 is characterized in the visible region by a broad band with the $\alpha$ band centered at 565 nm. A detailed analysis by a band-fitting program using Gaussian line shapes

of the absorption spectra (data not shown) revealed that the visible region of spectrum 1 (Figure 4) could be reproduced only by using a minimum number of four bands at about 524, 540, 556, and 570 nm, whereas spectrum 4 could be fitted with only two bands at 540 and 571 nm. The Soret region of both spectra was reproduced by using three bands at about 395, 407, and 422 nm, with different relative intensities on going from spectrum 1 to 4. Therefore, the band shape of the initial intermediate species is perfectly compatible with a mixture of (i) 5-c protoheme−CO, (ii) $H_2O$−protoheme−CO, and (iii) His−protoheme−CO, species ii converting to form iii at a rate likely limited by the dissociation of $H_2O$ from the proximal side [see Huang et al. (1991)]. However, the recovery of the peak absorption at 422 nm (see Figure 4) and thus the displacement of $H_2O$ from His on the proximal side of the heme pocket are not accompanied by a concomitant significant variation of the CD spectrum in the Soret region, which remains inverted with respect to that observed at pH 7.0 (see Figure 5). It suggests that pH lowering brings about a conformational change of the CO-bound heme in HRP and that the final absorption spectrum, though similar, does not correspond to the same species observed at pH 7.0. This is also confirmed by RR spectra reported in Figure 6, since they clearly show as well significant differences between spectra of HRP−CO at pH 7.0 and at pH 3.1. Therefore, even though the slow recovery of the absorption peak at 422 nm indeed may refer to the rebinding of His to heme's iron, the conformation of the His−heme−CO complex at pH 3.1 drastically differs from that predominant at pH 7.0. This latter has been interpreted as due to CO complexes with a hydrogen bond between the oxygen atom of the bound CO and a proton of a distal residue (Evangelista-Kirkup et al., 1986; Uno et al., 1987).

Even though the substitution of $H_2O$ by His on the proximal side of the heme pocket may be the slowest process along the pathway from the ferric form to the final His−heme−CO, there must be an additional rate-limiting step, since the observation by rapid-mixing technique of the process, beside the very slow process reported in Figure 4, shows the occurrence of an additional faster phase ($t_{1/2} \cong$ 100 ms), which is also independent of CO concentration (data not shown), and which leads from ferric to the metastable species (spectrum 1 of Figure 4) characterized by the increase of absorption at 422 nm and a decrease of absorption at 380 nm.

In agreement with the changes with time observed in the absorption spectra, two different CO complexes have been observed by the RR and IR experiments. The species which readily appears upon the CO complexation is characterized by the $\nu$(Fe−CO) and the $\nu$(CO) stretching modes at 526 (RR) and 1933 $cm^{-1}$ (IR) respectively; this form slowly converts to another, characterized by the $\nu$(Fe−CO) and the $\nu$(CO) stretching modes at 492 and 1967 $cm^{-1}$, respectively. The fact that the 526 $cm^{-1}$ band increases in intensity at the expense of the 492 $cm^{-1}$ upon blue-shifting of the excitation wavelength (from 413.1 nm vs 406.7 nm) confirms its origin from a Soret band at a wavelength lower than 422 nm. The same RR results have been previously obtained for the MbCO complex at acid pH. In this case no kinetics has been observed in the electronic absorption (Sage et al., 1991a), but a weak absorption peak near 410 nm was observed when the pH 3.8 spectrum was subtracted from the pH 2.5 spectrum. The same authors showed also that upon extended illumination the 526 $cm^{-1}$ peak increases in intensity at the expense of the 492 $cm^{-1}$ band. In addition, time-resolved RR experiments carried out under extended illumination showed that the iron−His mode was bleached from the spectrum of the five-coordinate photoproduct. These combined experiments allowed the authors to conclude that the proximal histidine ligand was replaced by a water molecule under continuous illumination (Sage et al., 1991b).

A similar intensity increase of the band at 526 $cm^{-1}$ is observed also for the HRP−CO complex upon extended illumination, giving rise to another indirect evidence that this species has lost its fifth histidine ligand. The Fe−CO stretching frequency of this species is identical to that observed either in the absence of the trans ligand or with weak ligands bound trans to CO of ferrous porphyrins (Yu & Kerr, 1988), but in these cases the corresponding CO stretching modes were observed at 1973 (no trans ligand) and 1957 $cm^{-1}$ (weak trans ligand), respectively (Wayland et al., 1978; Yu & Kerr, 1988).

A linear correlation, with a negative slope, between the frequency of the $\nu$(Fe−CO) and the $\nu$(CO) stretching modes has been found by several groups (Paul et al., 1985; Uno et al., 1987; Tsubaki et al., 1986; Yu & Kerr, 1988; Li & Spiro, 1988). The negative slope has been discussed in terms of back-donation in the Fe−CO unit. In fact, the interaction between the CO ligand and the Fe atom involves both $\sigma$ and $\pi$ bonding; in $\pi$ bonding the $d_\pi$ electrons of the metal are donated back to the empty $\pi^*$ orbitals of CO decreasing the C−O bond and increasing the Fe−C bond order. As a result, the frequency of the Fe−CO stretching mode increases while the frequency of the CO stretching mode decreases. The back-bonding is enhanced by many factors such as steric hindrance on the bound CO, polarity of the environment around the bound CO, and H-bonding between the oxygen atom of the bound CO and a proton of a distal residue. Large deviations from the above mentioned correlation are observed in the absence of the trans ligand or with trans ligands that are weaker donors than imidazole. In fact, in these cases back-bonding decreases, but the Fe−C $\sigma$ bond is strengthened (with a concomitant increase of the Fe−CO stretching mode frequency) due to less competition with the Fe $d_{z^2}$ orbitals (Li & Spiro, 1988).

In Figure 10 the $\nu$(Fe−CO) is plotted against $\nu$(CO) for CO adducts of a variety of heme proteins and model compounds having proximal histidine as fifth ligand (▲) or weaker/absent trans ligand (■). The frequencies of the stretching modes of the CO complexes are reported in Table 3.

From the figure it can be seen that the final form observed for HRP falls very close to that of Mb at acid pH ($A_0$ state, Ramsden & Spiro, 1989; Sage et al., 1991a,b), its mutant His(E7)Gly where the distal His was replaced with an apolar residue (Morikis et al., 1989; Lin et al., 1990), and to the model compound Fe−protoporphyrin IX dimethyl ester−ImH/CO in $CH_2Cl_2$ (Evangelista-Kirkup et al., 1986). The $A_0$ state of the Mb−CO adduct at acid pH has been correlated with an open distal pocket conformation resulting from the protonation of the distal imidazole (Breslow & Gurd, 1962; Puett, 1973, Sage et al., 1991a), which induces a swinging of the histidine side-chain out of the heme pocket (Quillin et al., 1992; Ray et al., 1994) leaving the Fe-CO unit in a nonpolar environment (Morikis et al., 1989). This has been

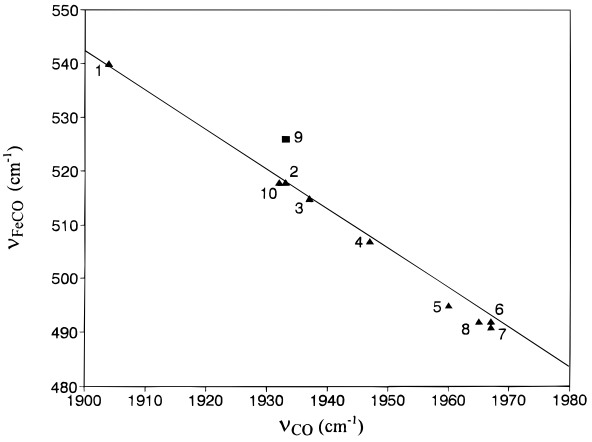


FIGURE 10: $\nu_{Fe-CO}$ vs $\nu_{CO}$ back-bonding correlations. The line is for proteins and model compounds in which the Fe−CO is ligated by histidine (▲). The (■) point represents HRP−CO complex at pH 3 with a trans ligand absent or weaker than imidazole. Frequencies are reported in Table 3.

Table 3: Vibrational Frequencies (cm$^{-1}$) of the FeCO Stretching Modes in CO adducts of Selected Iron Porphyrins and Heme Proteins

| molecule | $\nu$(Fe−CO) | $\nu$(CO) |
|---|---|---|
| 1. HRP, pH 7[a,b] | 540 | 1904 |
| 2. HRP, pH 7[b] | 518 | 1933 |
| 3. elephant Mb, pH 8.2[c] | 515 | 1937 |
| 4. sperm whale Mb, pH 7[d] | 507 | 1947 |
| 5. Fe(PPDME)(Im)[a] | 495 | 1960 |
| 6. HRP, pH 3 | 492 | 1967 |
| 7. sperm whale Mb, pH 3[e] | 491 | 1967 |
| 8. mutant Mb His(E7)GLY, pH 7[f] | 492 | 1965 |
| 9. HRP, pH 3 | 526 | 1933 |
| 10. sperm whale Mb, pH 7 and 3.9[f] | 518 | 1932 |

[a] Evangelista-Kirkup et al., 1986. [b] Uno et al., 1987. [c] Kerr et al., 1985. [d] Fuchsman and Appleby, 1979. [e] Sage et al., 1991a. [f] Morikis et al., 1989, Lin et al., 1990.

indeed recently shown to occur from the crystal structure of MbCO at acid pH (Yang & Phillips, 1996), and therefore, the HRP−CO adduct characterized by the 492 and 1967 cm$^{-1}$ bands is interpreted accordingly.

The initial HRP−CO form (point 9, Figure 10, Table 3) falls on the back-bonding correlation of proteins with imidazole as a fifth ligand, the $\nu$(CO) being about 25 cm$^{-1}$ lower than the corresponding mode observed for hemes with weak or absent trans ligands (Ray et al., 1994). Its signatures are very similar to those observed for the $A_3$ state of the Mb−CO adduct (Morikis et al., 1989) and are consistent with the existence of a tautomer of the distal His with the proton on the $N_\delta$ atom which, therefore, may donate the $N_\epsilon$ lone pair to the carbon atom of the bound CO (Ray et al., 1994).

Upon lowering the temperature the His−heme−CO species becomes predominant and very difficult to photolyze. This finding is not surprising considering that the decrease of temperature has been found to cause a strengthening of the ligands bound to the heme iron as a consequence of increased packing forces (Feis et al., 1994). In agreement with the previous finding for alkaline metMb at low temperature, also the Mb−CO complex shows an upshift of the core size marker bands upon lowering the temperature, indicating a slight contraction of the heme core.

Figure 11 shows a schematic description of the changes likely occurring for the heme ligation upon lowering the pH

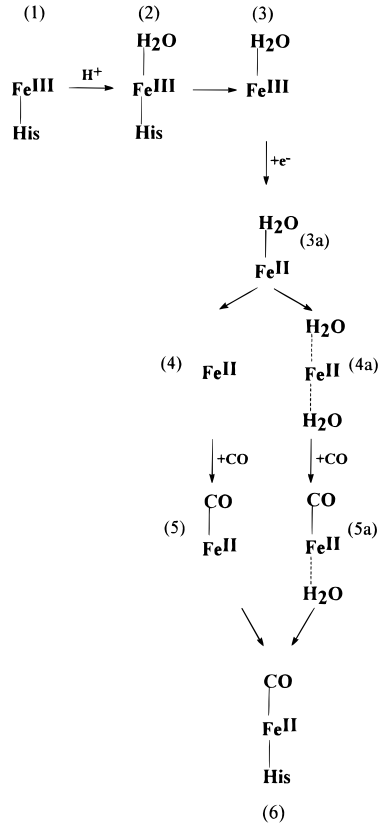


FIGURE 11: Possible heme−ligand structures for the ferric (**2** and **3**), ferrous (**3a**, **4**, and **4a**), and ferrous−CO complex (**5**, **5a**, and **6**) of HRP-C at acid pH. 1 represents the protein at neutral pH. For the sake of clarity the alternative form of **3** and **3a** with a water molecule bound on the proximal side of the iron heme is omitted.

from 7 to 3.1 and which might account for the spectroscopic observations reported throughout this paper. Upon acidification the five-coordinate native ferric form (**1**) converts to an intermediate six-coordinate species (**2**) followed by the loss of the proximal histidine (**3**). By reduction, the corresponding ferrous species (**3a**) may convert either to a four-coordinate species (**4**) or a bis−aquo−heme (**4a**). Therefore, binding of CO leads to a five-coordinate heme (**5**) and a six-coordinate CO−heme−aquo adduct (**5a**). Both species convert to the stable CO−Heme−His form, which is different from the species present at neutral pH.

## ACKNOWLEDGMENT

We thank Prof. Mario P. Marzocchi (Università di Firenze) for many helpful discussions.

## REFERENCES

Ascenzi, P., Brunori, M., Coletta, M., & Desideri, A. (1989) *Biochem. J. 258*, 473−478.

Blumberg, W. E., Peisach, J., Wittenberg, B. A., & Wittenberg, J. B. (1968) *J. Biol. Chem. 243*, 1854−1862.

Bosshard, H. R., Anni, H., & Yonetani, T. (1991) in *Peroxidases in Chemistry and Biology* (Everse, J., Everse, K. E., & Grisham, M. B., Eds.) Vol. II, pp 51−84, CRC Press, Boca Raton, FL.

Brault, D., & Rougee, M. (1974) *Biochemistry 13*, 4591−4597.

Cannon, J., Geibel, J., Whipple, M., & Traylor, T. G. (1976) *J. Am. Chem. Soc. 98*, 3395−3396.

Coletta, M., Ascenzi, P., Traylor, T. G., & Brunori, M. (1985) *J. Biol. Chem. 260*, 4151−4155.

Coletta, M., Ascoli, F., Brunori, M., & Traylor, T. (1986) *J. Biol. Chem. 261*, 9811−9814.

Dunford, H. B. (1991) in *Peroxidases in Chemistry and Biology* (Everse, J., Everse, K. E., & Grisham, M. B., Eds.) Vol. II, pp 1−24, CRC Press, Boca Raton, FL.
Eaton, W. A., & Hochstrasser, R. M. (1968) *J. Chem. Phys. 49*, 985−995.
Evangelista-Kirkup, R., Smulevich, G., & Spiro, T. G. (1986) *Biochemistry 25*, 4420−4425.
Feis, A., Paoli, M., Marzocchi, M. P., & Smulevich, G. (1994) *Biochemistry 34*, 4577−4583.
Fuchsman, W. H., & Appleby, C. A. (1979) *Biochemistry 18*, 1309−1321.
Giacometti, G. M., Traylor, T. G., Ascenzi, P., Brunori, M., & Antonini, E. (1977) *J. Biol. Chem. 252*, 7447−7448.
Han, S., Rousseau, D. L., Giacometti, G., & Brunori, M. (1990) *Proc. Natl. Acad. Sci. U.S.A. 87*, 205−209.
Holzbaur, I. E., English, A. M., & Ismail, A. A. (1996) *J. Am. Chem. Soc. 118*, 3354−3359.
Huang, Y., Marden, M. C., Lambry, J.-C., Fontaine-Aupart, M.-P., Pansu, R., Martin, J.-L., & Poyart, C. (1991) *J. Am. Chem. Soc. 113*, 9141−9144.
Iizuka, T., Makino, R., Ishimura, Y., & Yonetani, T. (1985) *J. Biol. Chem. 260*, 1407−1412.
Ikeda-Saito, M., Hori, H., Andersson, L. A., Prince, R. C., Pickering, I. J., George, G. N., Sanders, C. R., II., Lutz, R. S., McKelvey, E. J., & Mattera, R. (1992) *J. Biol. Chem. 267*, 22843−22852.
Kerr, E. A., Yu, N.-T., Bartnicki, D. E., Mizukami, H. (1985) *J. Biol. Chem. 260*, 8360−8365.
Kersten, P. J., Kalynaraman, B., Hammel, K. E., Reinhammar, B., & Kirk, T. K. (1990) *Biochem. J., 268*, 475-480.
Kertesz, D., Antonini, E., Brunori, M., Wyman, J., & Zito, R. (1965) *Biochemistry 4*, 2672−2676.
La Mar, G. N., & de Ropp, J. S. (1982) *J. Am. Chem. Soc. 104*, 5203−5206.
Li, X.-Y., & Spiro, T. G. (1988) *J. Am. Chem. Soc. 110*, 6024−6033.
Lin, S.-H, Yu, N.-T., Tame, J., Shih, D., Renaud, J.-P., Pagnier, J, & Nagai, K. (1990) *Biochemistry 29*, 5562−5566.
Maltempo, M. M. (1976) *Biochim. Biophys. Acta 434*, 513−518.
Meunier, B., Rodriguez-Lopez, J. N., Smith, A. W., Thorneley, R. N. F., & Rich, P. R. (1995) *Biochemistry 34*, 14687−14692.
Miller, M. A., Coletta, M., Mauro, J. M., Putnam, L. D., Farnum, M. F., Kraut, J., & Traylor, T. G. (1990a) *Biochemistry 29*, 1777−1791.
Miller, M. A., Mauro, J. M., Smulevich, G., Coletta, M., Kraut, J., & Traylor, T. G. (1990b) *Biochemistry 29*, 9978−9988.
Morikis, D., Champion, P. M., Springer, B. A., & Sligar, S. G. (1989) *Biochemistry 28*, 4791−4800.
Palaniappan, V., & Bocian, D. F. (1994) *Biochemistry 33*, 14264−14274.
Paul, J., Smith, M. L., & Paul, K.-G. (1985) *Biochim. Biophys. Acta 832*, 257−264.
Poulos, T. L. (1988) *Adv. Inorg. Biochem. 7*, 1−36.
Poulos, T. L., & Kraut, J. (1980) *J. Biol. Chem. 255*, 8199−8205.
Quillin, M. L., Brantley, R. E., Jr., Johnson, K. A., Olson, J. S., & Phillips, G. N., Jr. (1992) *Biophys. J. 61*, A446.
Quillin, M. L., Arduini, R. M., Olson, J. S., & Phillips, G. N., Jr. (1993) *J. Mol. Biol. 234*, 140−155.
Ramsden, J., & Spiro, T. G. (1989) *Biochemistry 28*, 3125−3128.
Ray, G. B., Li, X.-Y., Ibers, J. A., Sessler, J., & Spiro, T. G. (1994) *J. Am. Chem. Soc. 116*, 162−176.
Rougee, M., & Brault, D. (1973) *Biochim. Biophys. Res. Comm. 55*, 1364−1369.
Sage, J. T., Morikis, D., & Champion, P. M. (1991a) *Biochemistry 30*, 1228−1237.
Sage, J. T., Pusheng, L., & Champion, P. M. (1991b) *Biochemistry 30*, 1237−1247.
Sakurada, J., Takahashi, S., & Hosoya, T. (1986) *J. Biol. Chem. 261*, 9657−9662.
Sharonov, Y. A., Pismensky, V. F., & Yarmola, E. G (1988) *FEBS Lett. 235*, 63−66.
Smith, M. L., Ohlsson, P.-I., & Paul, K. G. (1983) *FEBS Lett. 163*, 303−305.
Smulevich, G., English, A. M., Mantini, A. R., & Marzocchi. M. P. (1991) *Biochemistry 30*, 772−779.
Smulevich, G., Paoli, M., Burke, J. F., Sanders, S. A., Thorneley, N. F., & Smith, A. T. (1994) *Biochemistry 33*, 7398−7407.
Smulevich, G., Neri, F., Willemsen, O., Choudhury, K., Marzocchi, M. P., & Poulos, T. L. (1995) *Biochemistry 34*, 13485−13490.
Traylor, T. G., Koga, N., & Deardurff, L. A. (1985) *J. Am. Chem. Soc. 107*, 6504−6510.
Tsubaki, M., Hitawatashi, A., & Ichikawa, Y. (1986) *Biochemistry 25*, 3563−3569.
Uno, T., Nishimura, Y., Tsuboi, M., Makino, R., Iizuka, T., & Ishimura, Y. (1987) *J. Biol. Chem. 262*, 4549−4556.
Vitello, L. B., Erman, J. E., Miller, M. A., Mauro, J. M., & Kraut, J. (1992) *Biochemistry 31*, 11524−11535.
Vitello, L. B., Erman, J. E., Miller, M. A., Wang, J., and Kraut, J. (1993) *Biochemistry 32*, 9807−9818.
Wayland, B. B., Mehne, L. F., & Swartz, J. (1978) *J. Am. Chem. Soc. 100*, 2379−2383.
Willick, G. E., Schonbaum, G. R., and Kay, C. M. (1969) *Biochemistry 8*, 3729−3734.
Yamada, H., & Yamazaki, I. (1977) *Arch. Biochem. Biophys. 171*, 737−744.
Yang, F., & Phillips, G. N., Jr. (1996) *J. Mol. Biol. 256*, 762−774.
Yu, N.-T., & Kerr, E. A. (1988) in *Applications of Raman Spectroscopy to Biological Systems* (Spiro, T. G., Ed.) pp 39−95, Wiley, New York.

BI960427B